Open access • Journal Article • DOI:10.1063/1.4922446

Resistance controllability and variability improvement in a TaOx-based resistive memory for multilevel storage application — Source link

Amit Prakash, Damien Deleruyelle, Jeonghwan Song, Marc Bocquet ...+1 more authors

Institutions: Pohang University of Science and Technology

Published on: 09 Jun 2015 - Applied Physics Letters (AIP Publishing)

Topics: Resistive random-access memory

Resistance controllability and variability improvement in a TaO x -based resistive memory for multilevel storage application

A. Prakash, D. Deleruyelle, J. Song, Marc Bocquet, H. Hwang

A. Prakash, D. Deleruyelle, J. Song, Marc Bocquet, H. Hwang. Resistance controllability and variability improvement in a TaO x -based resistive memory for multilevel storage application. Applied Physics Letters, American Institute of Physics, 2015, 106 (23), pp.233104. 10.1063/1.4922446 . hal-01737306

AUTHOR QUERY FORM

AIP Publishing	**Journal: Appl. Phys. Lett.** **Article Number: 021524APL**	**Please provide your responses and any corrections by annotating this PDF and uploading it according to the instructions provided in the proof notification email.**

Dear Author,

Below are the queries associated with your article; please answer all of these queries before sending the proof back to AIP. Please indicate the following:

Figures that are to appear as color online only (i.e., Figs. 1, 2, 3) ______________________________ (this is a free service).

Figures that are to appear as color online and color in print______________________ (a fee of $325 per figure will apply).

Article checklist: In order to ensure greater accuracy, please check the following and make all necessary corrections before returning your proof.

1. Is the title of your article accurate and spelled correctly?
2. Please check affiliations including spelling, completeness, and correct linking to authors.
3. Did you remember to include acknowledgment of funding, if required, and is it accurate?

Location in article	**Query / Remark: click on the Q link to navigate to the appropriate spot in the proof. There, insert your comments as a PDF annotation.**
AQ1	Please check that the author names are in the proper order and spelled correctly. Also, please ensure that each author's given and surnames have been correctly identified (given names are highlighted in red and surnames appear in blue).
AQ2	Ref. 14 was not cited in your original manuscript. We have inserted a citation for it in the sentence beginning "However, precise control over the…" Please carefully review our placement of the citation and confirm that it is correct. If it is not correct, mark the citation for deletion and specify where the citation for Ref. 14 should be inserted.
AQ3	Please provide date and month in Refs. 14 and 16.
AQ4	We were unable to locate a digital object identifier (doi) for Refs. 7, 8, 9, 13, and 18. Please verify and correct author names and journal details (journal title, volume number, page number, and year) as needed and provide the doi. If a doi is not available, no other information is needed from you. For additional information on doi's, please select this link: http://www.doi.org/.

Thank you for your assistance.

APPLIED PHYSICS LETTERS **106**, 000000 (2015)

Resistance controllability and variability improvement in a TaO_x-based resistive memory for multilevel storage application

AQ1 A. Prakash,[1,a),b)] D. Deleruyelle,[2,a)] J. Song,[1] M. Bocquet,[2] and H. Hwang[1,b)]
[1]*Department of Materials Science and Engineering, Pohang University of Science and Technology (POSTECH), 77 Cheongam-ro, Nam-gu, Pohang, 790-784, South Korea*
[2]*Im2np, UMR CNRS 7334, Aix-Marseille Université, Marseille, France*

(Received 16 April 2015; accepted 1 June 2015; published online xx xx xxxx)

In order to obtain reliable multilevel cell (MLC) characteristics, resistance controllability between the different resistance levels is required especially in resistive random access memory (RRAM), which is prone to resistance variability mainly due to its intrinsic random nature of defect generation and filament formation. In this study, we have thoroughly investigated the multilevel resistance variability in a TaO_x-based nanoscale (<30 nm) RRAM operated in MLC mode. It is found that the resistance variability not only depends on the conductive filament size but also is a strong function of oxygen vacancy concentration in it. Based on the gained insights through experimental observations and simulation, it is suggested that forming thinner but denser conductive filament may greatly improve the temporal resistance variability even at low operation current despite the inherent stochastic nature of resistance switching process. © *2015 AIP Publishing LLC*. [http://dx.doi.org/10.1063/1.4922446]

Resistive random access memory (RRAM) is one of the most promising next generation memory candidates especially for storage class memory applications due to its scalability, structural simplicity, and backend process compatible stackability.[1–3] In addition, TaO_x as a RRAM switching material have been found to be of commercial interest due to its superior material property as well as memory performance.[3–6] To fulfill the increasing demand for low cost and higher density memory, the most obvious way to increase the storage capacity is by decreasing the physical size of the device to a nanoscale dimensions, and in RRAM the scalability down to 10 nm has been demonstrated.[7,8] Other interesting approach is to stack the devices 3-dimensionally, for which two feasible architectures of crossbar and vertical RRAM are reported.[9] However, both the methods require complex experimental processes and may suffer from other limitations. Another alternative and simpler way to increase storage density is to use multilevel cell (MLC) storage technology, in which more than one bit per cell can be stored without further decreasing the physical device size.[10,11] However, precise control over the resistance of the different resistance levels should be assured for reliable MLC operation especially for RRAM, which is known to suffer from variability and reliability issues due to certain randomness in its switching process.[12–14] AQ2

In RRAM, MLC characteristics can be obtained by various methods such as by varying the switching current (or compliance current), where different levels of low resistance state (LRS) can be obtained due to change in the total number of constituent defects of the conductive filament (CF) or by controlling the maximum reset voltage during reset operation which can result different levels of high resistance state (HRS) due to variation in the gap between CF tip and metal electrode.[10,11] MLC behavior by varying the program/erase pulse width is also reported.[11] Although MLC properties can easily be obtained in RRAM, its successful implementation is dictated mainly by the ability to precisely control the resistance margin between the two resistance levels. One of the most critical factors, which can degrade this margin, is the switching cycle-to-cycle variability. Therefore, the feasible approaches to minimize it should be delved into through the enhanced understanding of the responsible factors. The origin of this variability is mainly related to the change in the total content of the oxygen vacancy defects present in the CF after each switching event.[12] This compositional variation in the conductive channel leads to the conductivity fluctuation. More fundamentally, it can be understood in terms of having different activation energy of defect migration due to the random location and different surroundings of the defects with in the conductive channel.

In this study, we aim to develop enhanced understanding on the variability issue through experimental observation and simulation studies and correlate it with the CF size and defect concentration in it. For this, we fabricated nanoscaled (<30 nm) RRAM devices with TaO_x as a switching material. Based on the analysis of experimental observations and simulation, a possible way to minimize the variability between resistance levels for reliable MLC operation is proposed. The results show that the temporal resistance variability may greatly be improved even at low switching current by forming denser filament with smaller size. Monte-Carlo calculations show good agreement with the experimental data.

The device was fabricated on a patterned substrate with 30 nm TiN bottom electrode (BE) in a planner type device structure [see the inset of Fig. 1(a)]. The TiN electrode was deposited by CVD and its sides were protected by 100 nm

---

[a)] A. Prakash and D. Deleruyelle contributed equally to this work.

[b)] Authors to whom correspondence should be addressed. Electronic addresses: amitknp@postech.ac.kr/amit.knp02@gmail.com and hwanghs@postech.ac.kr

0003-6951/2015/106(24)/000000/4/$30.00

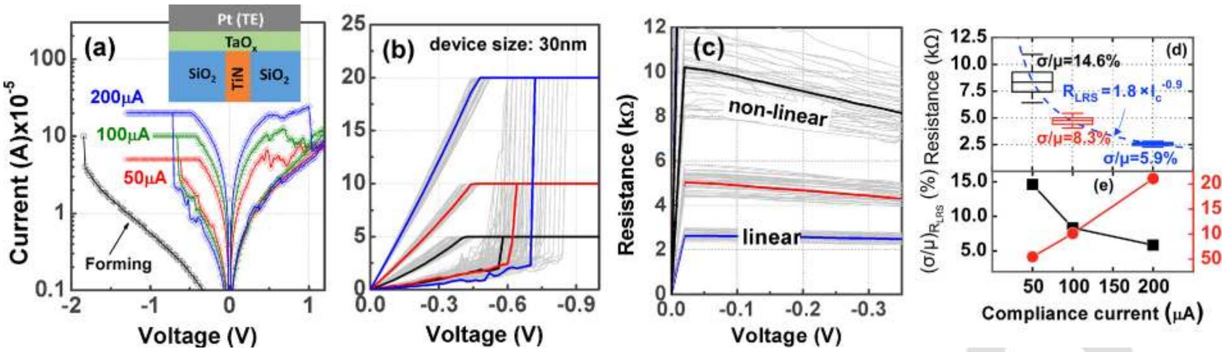

FIG. 1. (a) Forming and resistive switching behavior of fabricated 30 nm sized TaO_x-based resistive memory device with MLC characteristics. (b) Multiple MLC current-voltage (I-V) curves of all the LRS levels showing stable MLC characteristics. (c) Corresponding resistance-voltage (R-V) plot of all the low resistance levels confirming nonlinear conduction at smaller switching current. (d) Resistance of LRS and its distribution as a function of I_C. Both decrease with increasing I_C. (e) Evolution of LRS variability (σ/μ) and reset current (I_{reset}) with I_C.

thick SiO_2 layer. Tantalum oxide (TaO_x) switching layer of ~10 nm was deposited by reactive sputtering using Ta metal target and Ar+O_2 gases at room temperature. The rf power and working pressure were 100 W and 3 mTorr, respectively. Finally, inert (Pt) top electrode (TE) was sputter deposited on TaO_x switching layer. For electrical measurements, voltage was applied on TE and BE was connected to the ground.

Multilevel cell operation and resistance variability analysis of fabricated 30 nm size RRAM device is presented in Fig. 1. First, the device was formed by applying a negative voltage on Pt TE, as shown in Fig. 1(a). Small voltage of < -2.0 V was sufficient to form the device. After forming, the device exhibits resistive switching behavior and MLC characteristics by varying the switching current, as shown in Figs. 1(a) and 1(b). Multiple cycles for each level have been shown to ensure the stable resistance switching. Three different levels of LRS were obtained with same HRS, which can be used in 2-bit per cell storage. In addition, it was observed that the LRS current-voltage (I-V) gradually shifted from an ohmic to a nonlinear behavior as current compliance (I_C) was decreased down to 50 μA (Fig. 1(c)) due to decreased number of vacancy defects in the CF leading to the change in the current conduction mechanism. Simultaneously, the resistance margin between the resistance levels is reduced because of cycle-to-cycle resistance fluctuations. The resistance distribution of 50 consecutive cycles for each compliance is shown in Fig. 1(d), where the highest variability of 14.6% is observed for I_C of 50 μA. The read voltage was 0.25 V. Furthermore, the resistance of LRS (R_{LRS}) decreased with increasing I_C [Fig. 1(d)]. The slope of R_{LRS} vs I_C was found to be -0.9, which is close to the reported value of -1.[12] On the other hand, maximum reset current (I_{reset}) increases linearly and coefficient of variation (σ/μ) or variability of R_{LRS} decreases with increasing I_C, as shown in Fig. 1(e). The decrease in the variability is due to the increase in the number of oxygen vacancy defects in the CF with increasing I_C. Considering the dependence of LRS I-V nonlinearity on I_C and variability behavior, it can be said that by increasing I_C, both CF size and oxygen vacancy defect density in it may increase. In other words, R_{LRS} depends on filament size and its electrical conductivity.

The different electrical conduction behavior (linear/nonlinear) of the LRS I-V curves observed at different switching currents [Fig. 1(c)] can be understood by the oxygen vacancy concentration (n_{VO}) falling under a threshold value (n_{TAC}), which is the minimum concentration of oxygen vacancies below which trap assisted conduction (TAC) dominates and I-V becomes nonlinear, while above this concentration conduction is linear (ohmic).[15–18] This can be accounted by the following equation:

$$\sigma_e(n_{VO}) = \beta \times n_{V_o} \times \exp\left(-\frac{E_a(n_{V_o})}{kT}\right), \qquad (1)$$

$$\text{with} \quad E_a(n_{V_o}) = E_{a_0} \times f(n_{V_o}), \qquad (2)$$

where σ_e is the electrical conductivity, E_a is the activation energy, $\beta = 1 \times 10^{-23}\,\mathrm{S\,m^{-1}}$, k = Boltzmann constant, T = absolute temperature, and $E_{a0} = 0.4$ eV. This approach has already been employed to describe resistance switching phenomena or early data-retention failure in RRAM employing either HfO_x[15,16] or TaO_x.[17,18] The corresponding plot of σ_e as a function of n_{VO} is shown in Fig. 2. In the previous studies,[15–18] a piecewise linear and decreasing function f [Eq. (2)] was employed to account for the decrease of conduction activation energy at increasing defect concentrations which, in turns, increases σ_e in the CF region. Although a proper theoretical justification is still

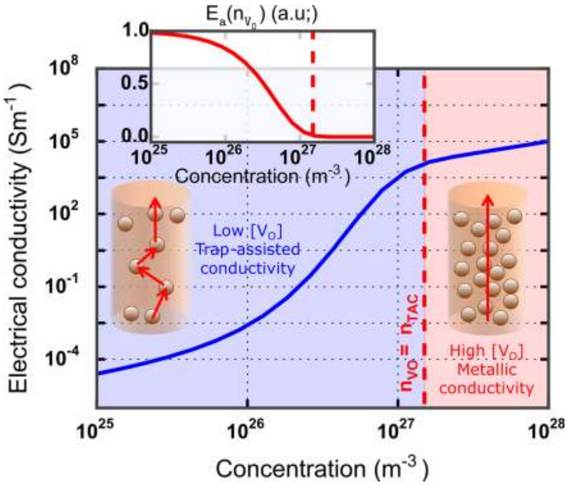

FIG. 2. Calculated electrical conductivity as function of oxygen vacancy concentration [Eq. (1)]. Inset shows the evolution of the activation energy with respect to n_{VO}.

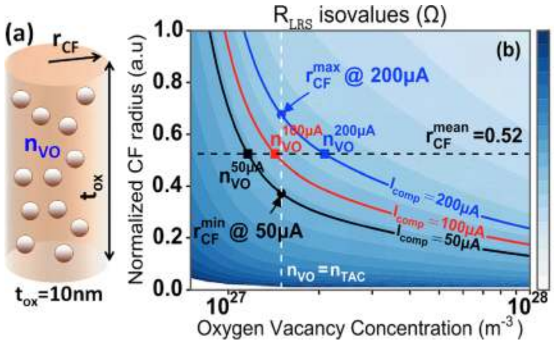

FIG. 3. (a) Schematic description of the conductive filament. (b) Maps of R_{LRS} as function of conductive filament radius and oxygen vacancy concentration. LRS isolines correspond to experimental mean LRS resistance values at different I_C.

lacking, this first-order approximation showed satisfactorily and quantitative agreement with data.[15,17,18] In this work, we employed a sigmoid function [see the inset of Fig. 2] rather than a piecewise linear function to describe the decreasing E_a with n_{V_O}. Although such a dependency is only justified as a piecewise decreasing function, it offers the numerical advantage of being indefinitely differentiable in the whole range of n_{V_O} to conduct further numerical or analytical studies. In the following, a value of n_{TAC} of $1.5 \times 10^{27}\,m^{-3}$ was employed (marked by vertical dashed line in Fig. 2), which corresponds to an inter-distance below 1 nm between oxygen vacancies. Considering the R_{LRS} equal to the resistance of CF (R_{CF}) in LRS and cylindrical filament [Fig. 3(a)], R_{CF} can be written as

$$R_{LRS} \approx R_{CF} = \left(\frac{1}{\sigma_e\,(n_{V_o})}\right) \times \left(\frac{t_{ox}}{(\pi \times r_{CF}^2)}\right), \qquad (3)$$

where t_{ox} is the oxide thickness (= 10 nm) and r_{CF} is the conductive filament radius. Figure 3(b) shows the R_{LRS} isovalue curves of all the resistance levels as a function of CF radius and oxygen vacancy concentration (n_{V_O}). The n_{V_O} equal to n_{TAC} is also shown by a dashed line. The dependence of R_{LRS} versus the vacancy concentration is intensified as the concentration falls below n_{TAC} (i.e., non-ohmic regime) as indicated by sharper R_{LRS} isovalues [Fig. 3(b)]. As vacancy generation and filament formation are intrinsically random in RRAM, vacancy concentration change in the filament is inevitable during cycle-to-cycle switching. Consequently, small changes in n_{V_O} may introduce large variability in the resistance of multilevel, in particular, when $n_{V_O} < n_{TAC}$ as observed in the experimental results [Fig. 1]. It is interesting to note that LRS variability not only depends on the filament radius (size) but also is strongly dictated by vacancy concentration and fluctuation in the filament. Interestingly, the graph also shows that the different topologies of filament (i.e., r_{CF} and n_{V_O}) can account for the experimental mean R_{LRS} values obtained at different I_C [Fig. 3]. Given the non-linearity (respectively, linearity) of I-V curves at 50 μA (respectively, 200 μA), r_{CF} can be reasonably assumed to be higher (respectively, lower) than r_{CF}^{min} (respectively, r_{CF}^{max}) to account for non-ohmic (respectively, ohmic) I-V.

To better understand the effect of vacancy concentration on the variability, let us assume a mean filament radius (r_{CF}^{mean}) in between r_{CF}^{min} and r_{CF}^{max}, as shown in Fig. 3(b) by horizontal dashed line. Three n_{V_O} can now be obtained on the R_{LRS} isovalue curves corresponding to switching currents of 50, 100, and 200 μA. Monte-Carlo calculations have been performed to reproduce the experimental LRS resistance distribution assuming a Gaussian distribution of n_{V_O} in Eq. (3). Results are presented in Figs. 4(a)–4(c). A pretty close match between the experimental variability data and calculations has been achieved using the values given in Figs. 4(d) and 4(e). It is interesting to note that a small (i.e., <5%) variation in n_{V_O} can result in a large (14.6%) variability in the resistance for 50 μA I_C and a 5.9% (smaller) resistance variation for 200 μA I_C. This underlines that the resistance variability is very sensitive to the n_{V_O} variation in the CF when it operates in the nonlinear region where electrical conductivity strongly depends on n_{V_O}. Conduction activation energies for each computed n_{V_O} are in the range between 0.8 meV (for Ic = 200 μA) and 16.7 meV (for Ic = 50 μA) [Fig. 4(e)]. E_a values are in the same order of magnitude than those already reported by Kim *et al.*[17,18] Figure 5 suggests possible way to

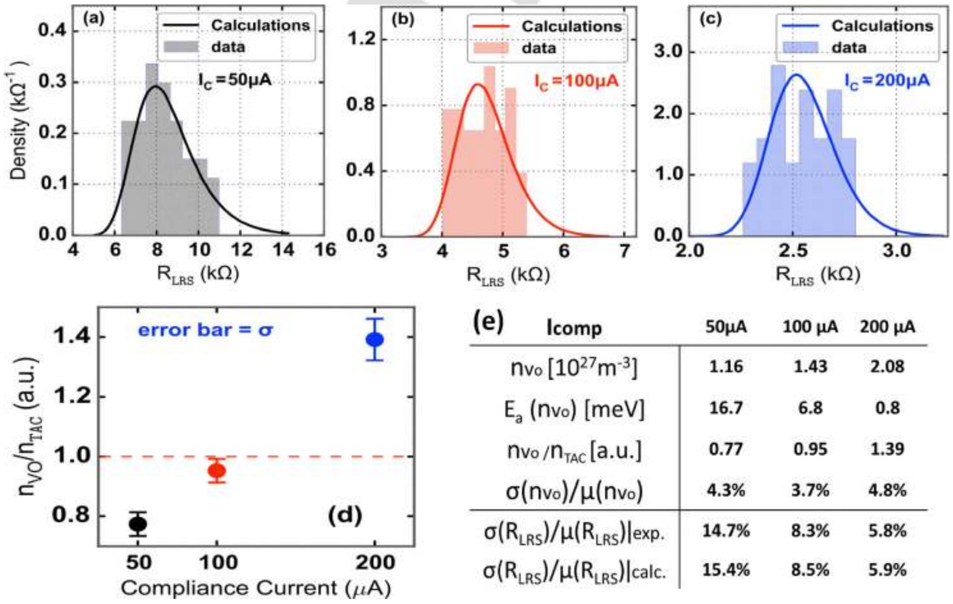

Icomp	50µA	100 µA	200 µA
n_{Vo} [$10^{27}m^{-3}$]	1.16	1.43	2.08
E_a (n_{Vo}) [meV]	16.7	6.8	0.8
n_{Vo}/n_{TAC} [a.u.]	0.77	0.95	1.39
$\sigma(n_{Vo})/\mu(n_{Vo})$	4.3%	3.7%	4.8%
$\sigma(R_{LRS})/\mu(R_{LRS})\vert_{exp.}$	14.7%	8.3%	5.8%
$\sigma(R_{LRS})/\mu(R_{LRS})\vert_{calc.}$	15.4%	8.5%	5.9%

FIG. 4. (a)–(c) Experimental normalized resistance distributions (histograms) and computed density (lines) for each I_C. Densities were computed using mean values and standard deviation of n_{vo} presented in (d). Table (e) is a summary of the experimental and calculation results.

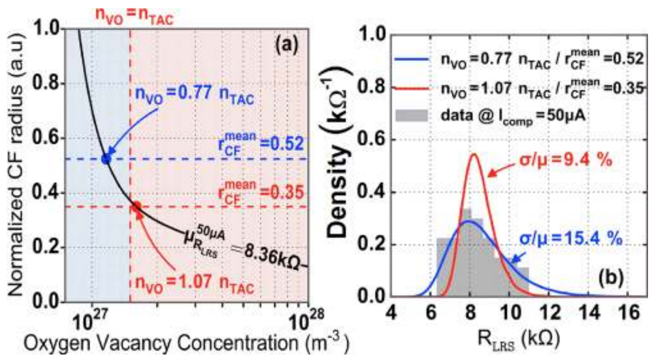

FIG. 5. (a) R_{LRS} isoline for $I_C = 50\,\mu A$. Shaded regions correspond to trap-assisted (left side) and ohmic (right side) transport regions. (b) Experimental (histogram) and computed resistance distribution (lines) using the same relative variation of n_{vo} for different n_{vo}/n_{TAC} values. It is shown that $n_{vo}/n_{TAC} > 1$ allows for smaller relative variation of R_{LRS}.

minimize the resistance variations even at low I_C. It is possible to improve the variations if we can shift to operate in the linear region instead of nonlinear region, as shown in Fig. 5(a). This can be achieved by generating smaller size filament with higher defect concentration. Calculations show that a tighter distribution with 8% variability can be achieved even at low I_C of 50 μA if n_{Vo}/n_{TAC} is increased from 0.77 to 1.07 in conjunction with r_{CF}^{mean} decreased from 0.52 to 0.35 [Fig. 5(b)]. Therefore, forming denser but thinner filament may remarkably improve the resistance fluctuation even at low operation current. Various techniques such as two step forming, material engineering, and different forming conditions can be exploited to generate different defect density filament.[6]

In this work, multilevel resistance variability was investigated on a nanoscale TaO_x-based RRAM operating in MLC mode by means of a theoretical approach assuming that non-linearity observed at low I_C is related to trap assisted conduction resulting from low concentration of oxygen vacancy. It was found that the resistance variability not only depends on the conductive filament size but also is a strong function of oxygen vacancy concentration and fluctuation, which is supported by Monte-Carlo calculations of LRS distributions at various compliance currents. Based on this study, it is suggested that LRS variability can be improved even at low I_C by forming denser CF in terms of oxygen vacancy by means of material engineering or dedicated forming techniques.

This work was supported by the POSTECH-Samsung Electronics ReRAM cluster research project.

[1] H. S. Philip Wong, H.-Y. Lee, S. Yu, Y.-S. Chen, Y. Wu, P.-S. Chen, B. Lee, F. T. Chen, and M.-J. Tsai, Proc. IEEE **100**, 1951 (2012).
[2] F. Pan, S. Gao, C. Chen, C. Song, and F. Zeng, Mater. Sci. Eng., R **83**, 1 (2014).
[3] A. Prakash, D. Jana, and S. Maikap, Nanoscale Res. Lett. **8**, 418 (2013).
[4] J. J. Yang, M. X. Zhang, J. P. Strachan, F. Miao, M. D. Pickett, R. D. Kelley, G. Medeiros-Ribeiro, and R. S. Williams, Appl. Phys. Lett. **97**, 232102 (2010).
[5] M. Lee, C. Lee, D. Lee, S. R. Lee, M. Chang, J. H. Hur, Y. B. Kim, C. J. Kim, D. H. Seo, S. Seo, U. I. Chung, I. K. Yoo, and K. Kim, Nat. Mater. **10**, 625 (2011).
[6] T. Ninomiya, Z. Wei, S. Muraoka, R. Yasuhara, K. Katayama, and T. Takagi, IEEE Trans. Electron Devices **60**, 1384 (2013).
[7] B. Govoreanu, G. S. Kar, Y.-Y. Chen, V. Paraschiv, S. Kubicek, A. Fantini, I. P. Radu, L. Goux, S. Clima, R. Degraeve, N. Jossart, O. Richard, T. Vandeweyer, K. Seo, P. Hendrickx, G. Pourtois, H. Bender, L. Altimime, D. J. Wouters, J. A. Kittl, and M. Jurczak, IEDM Tech. Dig. **2011**, 729. AQ4
[8] C. H. Ho, C.-L. Hsu, C.-C. Chen, J.-T. Liu, C.-S. Wu, C.-C. Huang, C. Hu, and F.-L. Yang, IEDM Tech. Dig. **2010**, 436.
[9] S.-G. Park, M. K. Yang, H. Ju, D.-J. Seong, J. M. Lee, E. Kim, S. Jung, L. Zhang, Y. C. Shin, I.-G. Baek, J. Choi, H.-K. Kang, and C. Chung, IEDM Tech. Dig. **2012**, 501.
[10] M.-C. Wu, W.-Y. Jang, C.-H. Lin, and T.-Y. Tseng, Semicond. Sci. Technol. **27**, 065010 (2012).
[11] S. Yu, Y. Wu, and H.-S. P. Wong, Appl. Phys. Lett. **98**, 103514 (2011).
[12] S. Ambrogio, S. Balatti, A. Cubeta, A. Calderoni, N. Ramaswamy, and D. Ielmini, IEEE Trans. Electron Devices **61**, 2912 (2014).
[13] S. Ambrogio, S. Balatti, A. Cubeta, A. Calderoni, N. Ramaswamy, and D. Ielmini1, IEDM Tech. Dig. **2013**, 782.
[14] A. Fantini, L. Goux, R. Degraeve, D. J. Wouters, N. Raghavan, G. Kar, A. Belmonte, Y.-Y. Chen, B. Govoreanu, and M. Jurczak, in *Proceedings of the IEEE International Memory Workshop*, ■ 2013, p. 30. AQ3
[15] S. Larentis, F. Nardi, S. Balatti, D. C. Gilmer, and D. Ielmini, IEEE Trans. Electron Devices **59**, 2468 (2012).
[16] T. Cabout, E. Vianello, E. Jalaguier, H. Grampeix, G. Molas, P. Blaise, O. Cueto, M. Guillermet, J. F. Nodin, L. Perniola, S. Blonkowski, S. Jeannot, S. Denorme, P. Candelier, M. Bocquet, and C. Muller, in *Proceedings of the IEEE International Memory Workshop*, ■ 2014, p. 22.
[17] S. Kim, S. Choi, and W. Lu, ACS Nano **8**, 2369 (2014).
[18] S. Kim, S.-J. Kim, K. M. Kim, S. R. Lee, M. Chang, E. Cho, Y.-B. Kim, C. J. Kim, U.-I. Chung, and I.-K. Yoo, Sci. Rep. **3**, 1680 (2013).